JREE: Vol. 10, No. 1, (Winter 2023) 59-67

Journal of Renewable Energy and Environment

Journal Homepage: www.jree.ir

Materials and Energy Research Center

MERC

Technical Note

Improving the Efficiency of a Cantilever Energy Scavenger

Mohammad Rahimzadeh [a*], Hamid Samadi [b], Nikta Shams Mohammadi [c]

[a] Department of Mechanical Engineering, Faculty of Engineering, Golestan University, P. O. Box: 49138-15759, Gorgan, Golestan, Iran.
[b] Department of Mechanical Engineering, Babol University of Technology, P. O. Box: 47148-73113, Babol, Mazandaran, Iran.
[c] Department of Electrical Engineering, Shahrood University of Technology, P. O. Box: 36199-95161, Shahrood, Semnan, Iran.

PAPER INFO

Paper history:
Received: 16 December 2021
Revised in revised form: 01 May 2022
Scientific Accepted: 21 May 2022
Published: 27 August 2022

Keywords:
Piezoelectric,
Cantilever Beam,
Energy Harvesting,
Voltage,
Unimorph

ABSTRACT

Energy harvesting from ambient vibrations using piezoelectric cantilevers is one of the most popular mechanisms for producing electrical energy. Recently, efforts have been made to improve the performance of energy harvesters. The output voltage dramatically depends on the geometrical and physical parameters of these devices. In addition, improved performance is often achieved by operating at or near the resonance point. So, this paper aims to reduce the natural frequency to match the environmental excitation frequency and increase the harvested energy. For this purpose, different geometrical and physical parameters are studied to determine the impact of each parameter. These parameters include the length, thickness, density, and Young's modulus of each layer. The beam is considered a unimorph cantilever with rectangular configuration and the study is performed using COMSOL Multiphysics software. The results are compared with those obtained by an analytical approach. The results show that changing the parameters made the natural frequency of the system vary in the range of 20 Hz to 200 Hz and increased the output voltage up to 20 V.

https://doi.org/10.30501/jree.2022.320113.1300

1. INTRODUCTION

Rapid advances in electronic devices and sensors have intensified the efforts for portable energy sources [1]. The high costs of constant battery replacement and the limited final weights of devices have increased the attempts at supplying energy from ambient vibrations such as vibration of the wing of a UAV during flight, traffic and wind induced vibrations in tall bridges, vibration coming from rotating tires of a vehicle, heart beats and blood pressure fluctuations in the human body, and vibration due to walking or physical exercise [2]. In general, mechanical energy can be converted into electrical energy through three mechanisms, namely electromagnetic [3], electrostatic, and piezoelectric [4]. At the same time, piezoelectric materials have been considered for use to boost the output voltage because they need no electrical sources [5].

The capability to harvest energy from the environment is significant, especially in high-tech industries like aerospace. For instance, Eugeni et al. [6] modeled a piezoelectric energy harvester on a fluid stream and developed it for use in wireless sensors. In another study, Liu et al. [7] developed energy harvesting arrays consisting of several piezoelectric elements to monitor traffic and energy harvesting. These arrays were examined to simulate the effects of loads and speeds of different vehicle axles. The impacts of piezoelectric configurations on the harvested amount of energy were then studied. The impacts of temperature on the output signals of the arrays were also analyzed. The experimental results indicated that the output voltage increased gradually as the load and frequency increased. With rapid developments in artificial intelligence technologies and the Internet of Things, wearable electronic devices have attracted a great deal of attention. Piezoelectric-based nanogenerators have great potential for use as human health monitoring sensors and biomechanical energy harvesters in wearable electronics due to their high flexibility, low weight, high reliability, and high accuracy [8, 9]. Piezoelectric materials are used as actuators, sensors, and energy harvesters in various medical devices. Natural piezoelectric materials have different properties from mineral piezoelectric materials. The high mechanical properties and flexibility of natural piezoelectric materials are very important and practical in various applications of medical equipment. Natural piezoelectric materials are used in medical sensors, which are located close to internal organs such as the heart due to the need for proper flexibility [10]. As discussed earlier, the exceptional capabilities and properties of piezoelectric materials have made them easy to use in different fields [11]. However, it is necessary to know everything about the field of use, limitations, and conditions of the system for the application of piezoelectric materials [12]. Hence, the parameters of energy harvesting systems must be appropriately designed [13].

*Corresponding Author's Email: m.rahimzadeh@gu.ac.ir (M. Rahimzadeh)
URL: https://www.jree.ir/article_155304.html

Please cite this article as: Rahimzadeh, M., Samadi, H. and Shams Mohammadi, N., "Improving the efficiency of a cantilever energy scavenger", ***Journal of Renewable Energy and Environment (JREE)***, Vol. 10, No. 1, (2023), 59-67. (https://doi.org/10.30501/jree.2022.320113.1300).

In the conventional design of energy scavengers based on piezoelectric materials, a cantilever beam configuration is used with a piezoelectric layer [14]. Creating high strain energy and reducing natural frequencies in this configuration are the main reasons for employing such a beam to harvest energy [15]. Nevertheless, the natural frequencies in these mechanisms range from several hundred Hz to several kHz. Of note, the excitation frequencies of environmental resources are usually not very high. A way of solving this problem is to use proof mass at the free end of the beam. This method helps reduce the resonant frequency of the energy harvesting system [16]. Moreover, the geometry of the beam structure and properties of the materials used have substantial impacts on an energy harvesting performance [17]. In recent studies, beams have been used in various geometrical shapes such as rectangular and triangular shapes. Moreover, it is possible to increase the harvested energy by applying optimization methods to the geometrical parameters of the beams [18]. The output power depends significantly on the properties of materials and the geometrical parameters of the beam [19]. Stress and strain increase as the geometrical properties of the beam change; therefore, higher levels of voltage and power can be harvested from a specific piezoelectric material [20]. According to the research results, the natural frequency of a triangular beam is lower than that of a rectangular or trapezoidal beam under the same conditions. Furthermore, the thickness of the beam layer affects the performance of an energy harvester performance. The beam structure is usually in the form of an elastic layer with a piezoelectric patch (unimorph) or an elastic layer with two piezoelectric patches on either side of the elastic layer (bimorph) [21, 22].

An energy harvesting system must be appropriately designed in an environment exposed to ambient vibrations due to the adaption of that system to environmental conditions. Efficiency improvement is important in the design and analysis of energy harvesters. Efficiency is defined as the ratio of the output electrical energy to the input mechanical energy. Despite several studies on the efficiency analysis of energy harvesters, the effects of geometric and physical parameters on the performance of energy harvesters have not been explored simultaneously through analytical and numerical (FEM) approaches. In this study, different multiplication factors were applied to geometrical and physical parameters such as beam length, thickness, density, and Young's modulus to measure the effect of each on the energy harvesting process. The resulting information of these simulations can lead to a more appropriate design of an energy scavenger. Based on the separate analysis of the effect of each parameter on the energy harvesting process, it is possible to select the appropriate material and geometry of the energy harvester to meet the needs and conditions of each environment. The energy harvester beam was considered rectangular and unimorph.

2. ELECTROMECHANICAL MODEL OF THE ENERGY HARVESTER

One of the most common models of energy harvesting is a cantilever beam with a piezoelectric layer, which is shown in Figure 1. The beam has the width of b and length of L. It also consists of an elastic layer with the thickness of h_s and a piezoelectric layer with the thickness of h_p. The electrodes cover the entire surface of the piezoelectric layer, which does not slip with respect to the beam.

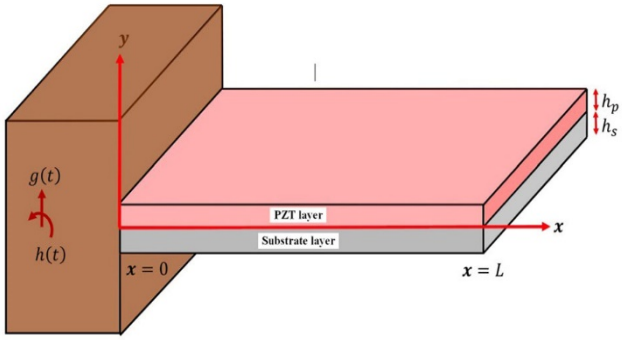

Figure 1. The schematic view of an energy scavenger under base vibrations

The general motion of the beam under forced vibrations including the base motion and its transverse displacements can be expressed as in Equation 1 [23]:

$$w(x,t) = w_b(x,t) + w_r(x,t) \tag{1}$$

where $w_b(x,t)$ is the motion of the base of the beam and $w_r(x,t)$ is the transverse displacement of the beam related to the clamped end. Moreover, the motion of the beam base is defined as in the following equation:

$$w_b(x,t) = g(t) + xh(t) \tag{2}$$

where $g(t)$ is the translational motion of the beam along the Y-axis and $h(t)$ is the rotation of the beam around the Z-axis. The equation of motion assuming the Euler-Bernoulli beam theory can be expressed as follows [23]:

$$\frac{\partial^2 M(x,t)}{\partial x^2} + C_s I \frac{\partial^5 w_{rel}(x,t)}{\partial x^4\,\partial t} + C_a \frac{\partial w_{rel}(x,t)}{\partial t} + m\frac{\partial^2 w_{rel}(x,t)}{\partial t^2} = -m\frac{\partial^2 w_b(x,t)}{\partial t^2} - C_a \frac{\partial w_b(x,t)}{\partial t} \tag{3}$$

The bending moment $M(x,t)$ is calculated as follows:

$$M(x,t) = -\int_{h_a}^{h_b} T_1^s b\,y\,dy - \int_{h_b}^{h_c} T_1^p b\,y\,dy \tag{4}$$

where T_1^s and T_1^p denote stress in the elastic and piezoelectric layers, respectively.

$$T_1^s = Y_s S_1^s \tag{5}$$

$$T_1^p = Y_p(S_1^p - d_{31}E_3) \tag{6}$$

where d_{31} refers to the piezoelectric constant and E_3 denotes the electric field, whereas S_1^s indicates the strain in the elastic layer. Furthermore, S_1^p shows the strain in the piezoelectric layer. Replacing the values obtained in Equation 4 yields the following equations:

$$M(x,t)=\int_{h_a}^{h_b} Y_s b\frac{\partial^2 w_{rel}(x,t)}{\partial x^2}y^2\,dy+\int_{h_b}^{h_c} Y_p b\frac{\partial^2 w_{rel}(x,t)}{\partial x^2}y^2\,dy-\int_{h_b}^{h_c} v(t)Y_p b\frac{d_{31}}{h_p}y\,dy \quad (7)$$

$$M(x,t)=YI\frac{\partial^2 w_{rel}(x,t)}{\partial x^2}+\vartheta v(t) \quad (8)$$

where Y_s denotes Young's modulus of the substrate layer, Y_p Young's modulus of the piezoelectric material, I the moments of inertia of the beam cross-section, and m the linear mass density of the beam. The bending stiffness of the composite beam and electromechanical coupling can be obtained from the following equations:

$$YI=b\left[\frac{Y_s(h_b^3-h_a^3)+Y_p(h_c^3-h_b^3)}{3}\right] \quad (9)$$

$$\vartheta=-\frac{Y_p d_{31} b}{2h_p}(h_c^2-h_b^2) \quad (10)$$

$$M(x,t)=YI\frac{\partial^2 w_{rel}(x,t)}{\partial x^2}+\vartheta v(t)[H(x)-H(x-L)] \quad (11)$$

Figure 2 demonstrates the beam cross-section.

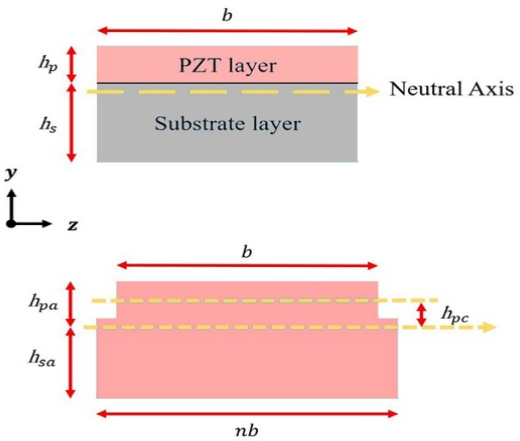

Figure 2. The cross-section of an energy scavenger and it's equivalent cross-section

The following equations can be employed to find the position of the neutral axis [23]:

$$n=\frac{Y_s}{Y_p} \quad (12)$$

$$h_{pa}=\frac{{h_p}^2+2nh_ph_s+n{h_s}^2}{2(h_p+nh_s)} \quad (13)$$

$$h_{sa}=\frac{{h_p}^2+2h_ph_s+n{h_s}^2}{2(h_p+nh_s)} \quad (14)$$

$$h_{pc}=\frac{nh_s(h_p+h_s)}{2(h_p+nh_s)} \quad (15)$$

To maintain the relationship between electrical and mechanical parameters of the system, it is necessary to define the piezoelectric constitutive relations [24]:

$$D_3=d_{31}T_1+\varepsilon_{33}^T E_3 \quad (16)$$

$$D_3(x,t)=d_{31}Y_pS_1(x,t)-\varepsilon_{33}^S\frac{v(t)}{h_p} \quad (17)$$

$$S_1(x,t)=-h_{pc}\frac{\partial^2 w_{rel}(x,t)}{\partial x^2} \quad (18)$$

$$D_3(x,t)=-d_{31}Y_ph_{pc}\frac{\partial^2 w_{rel}(x,t)}{\partial x^2}-\varepsilon_{33}^S\frac{v(t)}{h_p} \quad (19)$$

In the above equations, D_3 refers to the electric displacement, whereas ε_{33}^T represents the permittivity, and E_3 denotes the electric field. Moreover, current $i(t)$ and voltage $v(t)$ can be calculated in accordance with the amount of electric charge $q(t)$.

$$q(t)=\int_A D.\,ndA=-\int_{x=0}^{L}\left(d_{31}Y_ph_{pc}\frac{\partial^2 w_{rel}(x,t)}{\partial x^2}+\varepsilon_{33}^S b\frac{v(t)}{h_p}\right)dx \quad (20)$$

$$i(t)=\frac{dq(t)}{dt}=-\int_{x=0}^{L} d_{31}Y_ph_{pc}b\frac{\partial^3 w_{rel}(x,t)}{\partial x^2\,\partial t}dx-\frac{\varepsilon_{33}^S bL}{h_p}\frac{dv(t)}{dt} \quad (21)$$

$$\frac{\varepsilon_{33}^S bL}{h_p}\frac{dv(t)}{dt}+\frac{v(t)}{R_l}=-\int_{x=0}^{L} d_{31}Y_ph_{pc}b\frac{\partial^3 w_{rel}(x,t)}{\partial x^2\,\partial t}dx \quad (22)$$

$$v(t)=R_li(t)=-R_l\left[\int_{x=0}^{L} d_{31}Y_ph_{pc}b\frac{\partial^3 w_{rel}(x,t)}{\partial x^2\,\partial t}dx-\frac{\varepsilon_{33}^S bL}{h_p}\frac{dv(t)}{dt}\right] \quad (23)$$

In the above equations, h_{pc} refers to the distance between neutral axis and the piezoelectric layer center, whereas R_l indicates the electrical resistance of the circuit. To solve the

governing equations, the transverse motion of the beam can be written as a convergent series of eigenfunctions:

$$w_{rel}(x,t) = \sum_{r=1}^{n} \emptyset_r(x)\,\eta_r(t) \tag{24}$$

$$\emptyset_r(x) = \sqrt{\frac{1}{ml}}\left[\cosh\frac{\lambda_r}{L}x - \cos\frac{\lambda_r}{L}x - \sigma_r\left(\sinh\frac{\lambda_r}{L}x - \sin\frac{\lambda_r}{L}x\right)\right] \tag{25}$$

$$\eta_r(t) = \frac{[m\omega^2(\gamma_r^w Y_0 + \gamma_r^\theta \theta_0) - \chi_r V_0]e^{j\omega t}}{\omega_r^2 - \omega^2 + j2\zeta_r\omega_r\omega} \tag{26}$$

where $\emptyset_r(x)$ represents the mass normalized eigenfunction, and $\eta_r(t)$ indicates the modal coordinate of the cantilever beam. Herein, λ_r's can be specified by solving the characteristic equation:

$$1 + \cos\lambda\cosh\lambda = 0 \tag{27}$$

$$\sigma_r = \frac{\sinh\lambda_r - \sin\lambda_r}{\cosh\lambda_r + \cos\lambda_r} \tag{28}$$

where:

$$\omega_r = \lambda_r^2\sqrt{\frac{YI}{mL^4}} \tag{29}$$

$$\gamma_r^w = \int_0^L \emptyset_r(x)\,dx \tag{30}$$

$$\gamma_r^\theta = \int_0^L x\emptyset_r(x)\,dx \tag{31}$$

Assuming:

$$h(t) = \theta_0 e^{j\omega t} \tag{32}$$

$$g(t) = Y_0 e^{j\omega t} \tag{33}$$

$$v(t) = V_0 e^{j\omega t} \tag{34}$$

$v(t)$ can be defined as follows:

$$V_0 = \frac{\sum_{r=1}^{\infty}\frac{jm\omega^3\varphi_r(\gamma_r^w Y_0 + \gamma_r^\theta\theta_0)}{\omega_r^2-\omega^2+j2\zeta_r\omega_r\omega}}{\sum_{r=1}^{\infty}\frac{j\omega\chi_r\varphi_r}{\omega_r^2-\omega^2+j2\zeta_r\omega_r\omega} + \frac{1+j\omega\tau_c}{\tau_c}} \tag{35}$$

$$v(t) = \frac{\sum_{r=1}^{\infty}\frac{jm\omega^3\varphi_r(\gamma_r^w Y_0 + \gamma_r^\theta\theta_0)e^{j\omega t}}{\omega_r^2-\omega^2+j2\zeta_r\omega_r\omega}}{\sum_{r=1}^{\infty}\frac{j\omega\chi_r\varphi_r}{\omega_r^2-\omega^2+j2\zeta_r\omega_r\omega} + \frac{1+j\omega\tau_c}{\tau_c}} \tag{36}$$

$$\frac{v(t)}{-\omega^2 Y_0 e^{j\omega t}} = \frac{\sum_{r=1}^{\infty}\frac{-jm\omega\varphi_r\gamma_r^w}{\omega_r^2-\omega^2+j2\zeta_r\omega_r\omega}}{\sum_{r=1}^{\infty}\frac{j\omega\chi_r\varphi_r}{\omega_r^2-\omega^2+j2\zeta_r\omega_r\omega} + \frac{1+j\omega\tau_c}{\tau_c}} \tag{37}$$

where:

$$\varphi_r = -\frac{d_{31}Y_p h_{pc} h_p}{\varepsilon_{33}^s L}\int_{x=0}^{L}\frac{d^2\emptyset_r(x)}{dx^2}dx = -\frac{d_{31}Y_p h_{pc} h_p}{\varepsilon_{33}^s L}\frac{d\emptyset_r(x)}{dx}\Big|_{x=L} \tag{38}$$

3. PROBLEM STATEMENT

Table 1 presents the geometrical and mechanical characteristics of the unimorph beam. To study the effects of scavenger parameters such as length, thickness, Young modulus, and density on lowest resonant frequency and harvester performance, a comparative study has been carried out by considering some multiplication factors. Better insight can be achieved by multiplying each parameter by factors 0.5, 1, and 1.5, whereas others are deemed to be constant. This approach, for the design of an energy scavenger, leads to a more appropriate selection of materials and geometrical properties. Hence, it is possible to obtain a greater amount of energy. The numerical simulations were performed in COMSOL Multiphysics software (Figure 3). Additionally, the load resistance was considered $R_l = 10^6\ \Omega$ in this study.

Table 1. The mechanical and geometrical characteristics of the piezoelectric and substrate layers

Parameter	Substrate layer	PZT layer
Young modulus (GPa)	100	66
Density (Kg/m3)	7165	7800
Length (mm)	100	100
Width (mm)	20	20
Thickness (mm)	0.5	0.4

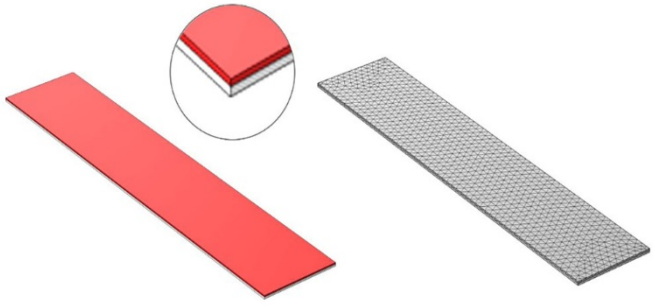

Figure 3. The geometrical and meshed model of the rectangular beam

4. RESULTS AND DISCUSSION

Table 2 shows the analytical and numerical (COMSOL) natural frequencies of the harvester. As can be seen, the

results are in good agreement. The numerical first natural frequency was found to be 47.82 Hz in COMSOL, whereas it was analytically calculated to be 47.81 Hz. Figure 4 depicts the numerical mode shapes 1-3 of the energy scavenger. Figure 5 plots the analytical output voltage at 0-400 Hz for resistive loads of 500 Ω, 5 kΩ, and 50 kΩ logarithmically. As can be seen, the output voltage was maximized at the natural frequencies. In addition, a rise in the resistive load raised the output voltage. This is evident throughout the frequency range, including the second natural frequency. Figure 6 depicts the numerical output voltage of the harvester at 0-400 Hz for the same resistive loads in COMSOL. The logarithmic voltage was obtained to be -0.938, -0.012, and 0.576 V at resistive loads of 500 Ω, 5 kΩ, and 50 kΩ, respectively, at the first natural frequency. At the second natural frequency, however, the logarithmic voltage was found to be -1.501, -0.650, and -0.325 V at resistive loads of 500 Ω, 5 kΩ, and 50 kΩ, respectively. Figure 7 compares the numerical and analytical output voltages at 0-400 Hz for a resistive load of 50 kΩ. As can be seen, the numerical and analytical results were in good agreement. The slight difference between the output voltage results at the second natural frequency arose from the use of a constant damping ratio throughout the frequency range in the numerical model in COMSOL.

Table 2. Comparing the values of natural frequencies obtained from COMSOL Multiphysics and MATLAB

	COMSOL Multiphysics	**Matlab**
1st natural frequency (Hz)	47.82	47.81
2nd natural frequency (Hz)	299.65	299.61
3rd natural frequency (Hz)	838.81	838.92

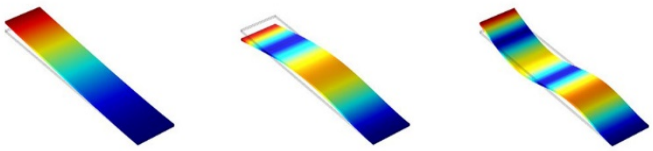

Figure 4. The first three mode shapes of the unimorph cantilever scavenger

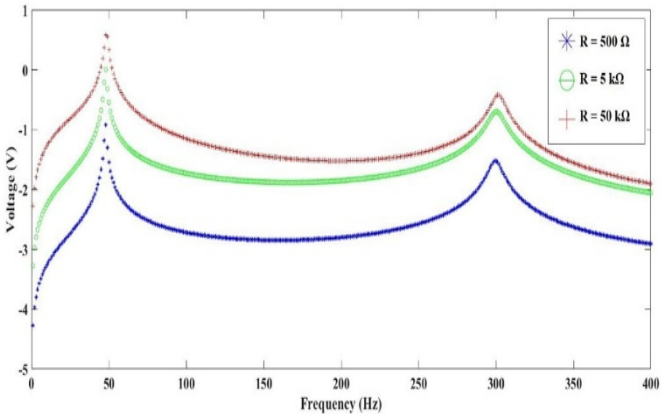

Figure 5. The voltage output versus the frequency for the unimorph cantilever beam within the range of 0 to 400 Hz through the analytical method

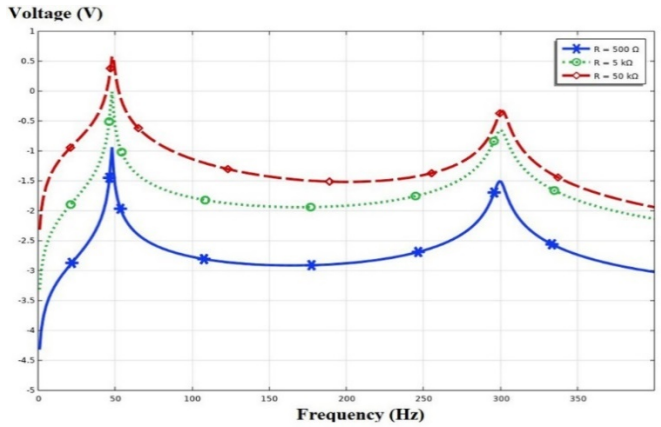

Figure 6. The voltage output versus the frequency for the unimorph cantilever beam within the range of 0 to 400 Hz from COMSOL Multiphysics

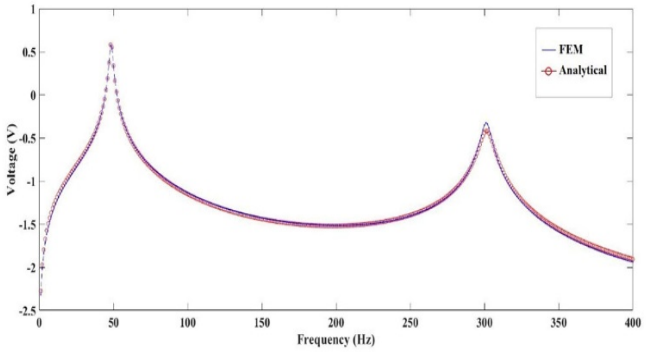

Figure 7. The voltage output versus the frequency for the unimorph cantilever beam within the range of 0 to 400 Hz for $R_l = 50$ kΩ through the analytical method and simulation from COMSOL Multiphysics

Figure 8 plots the analytical output voltage for 10-210 Hz at a resistive load of 1 MΩ and different lengths. As can be seen, a 50 % reduction (increase) in the initial harvester length (i.e., 100 mm) reduced (increased) the output voltage and increased (reduced) the natural frequency. Since ambient vibration typically occurs at low frequencies, an increase in the beam length would enhance harvester performance. Figure 9 depicts the numerical output voltage for 10-210 Hz at a resistive load of 1 MΩ and different lengths. According to Figure 9, the numerical output voltage was calculated to be 2.921, 10.679, and 22.423 V at length factors of 0.5, 1.0, and 1.5, respectively; a rise in the energy scavenger length from 100 to 150 mm led to a 110 % increase in the output voltage. The numerical results show good agreement with the analytical calculations.

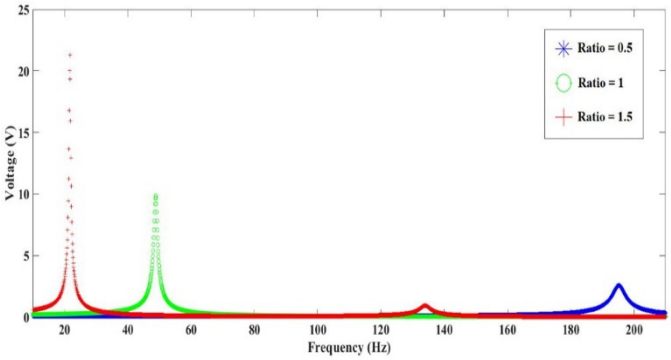

Figure 8. The voltage versus the frequency for variations in the beam length through the analytical method

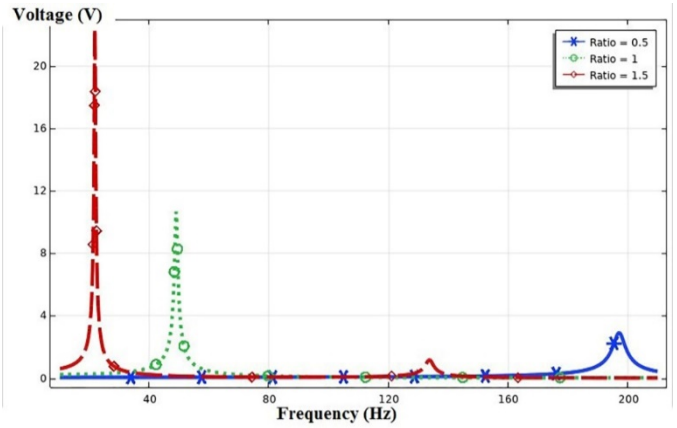

Figure 9. The voltage versus the frequency for variations in the beam length through the finite elements

Figure 10 plots the analytical output voltage at 30-70 Hz for substrate layer thicknesses of 0.25, 0.50, and 0.75 mm (ratios 0.5, 1.0, and 1.5). As shown in Figure 10, a reduction in the substrate thickness diminished the natural frequency and elevated the output voltage of the energy scavenger. Although the decreased substrate thickness led to only a slight rise in the output voltage, it could be considered for performance improvement as the natural frequency of the energy scavenger would substantially decline. The output voltage was maximized (8.8 V) at a substrate thickness of 0.75 mm. Figure 11 plots the analytical output voltage at 35-65 Hz for piezoelectric layer thicknesses of 0.2, 0.4, and 0.6 mm (factors 0.5, 1.0, and 1.5). As can be seen, a decrease (rise) in the thickness of the piezoelectric layer decreased (raised) the output voltage and reduced (increased) the natural frequency of the harvester. This is not efficient in the performance improvement of the harvester as the output voltage undergoes a small rise, while the natural frequency substantially increases.

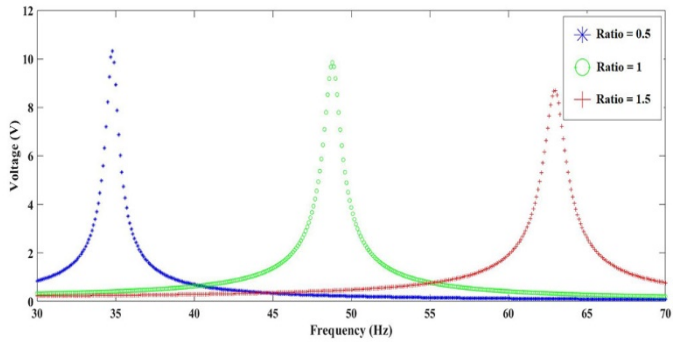

Figure 10. The voltage versus the frequency for variations in the substrate thickness through the analytical method

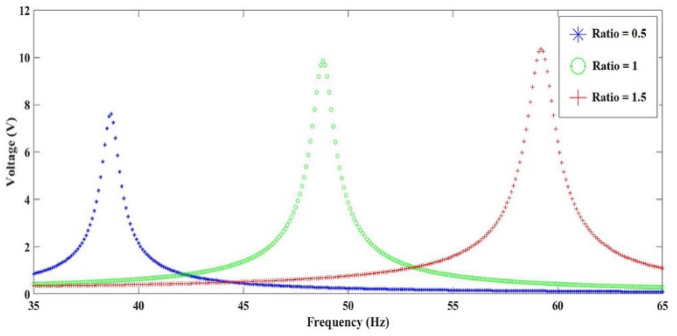

Figure 11. The voltage versus the frequency for variations of the piezoelectric layer thickness through the analytical method

Figure 12 shows the numerical output voltage at 35-65 Hz for piezoelectric layer thicknesses of 0.2, 0.4, and 0.6 mm (ratios 0.5, 1.0, and 1.5). The numerical results were in good agreement with the analytical calculations. The maximum numerical output voltage was found to be 9.338 V at a piezoelectric layer thickness of 0.2 mm.

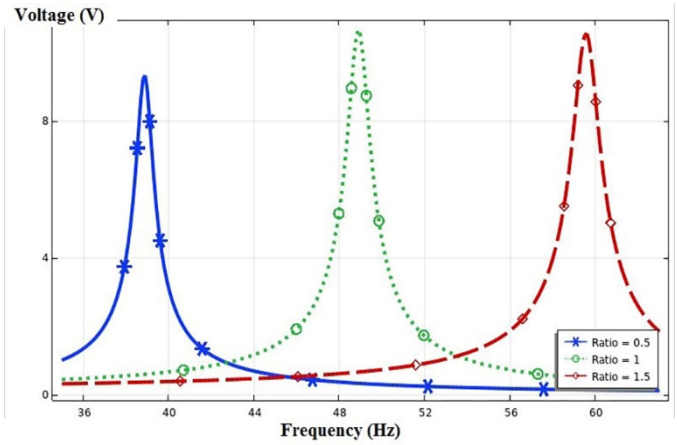

Figure 12. The generated voltage versus the frequency for variations of the piezoelectric layer thickness from COMSOL Multiphysics

Figure 13 represents the analytical output voltage at 40-55 Hz for substrate elasticity moduli of 50, 100, and 150 GPa (ratios 0.5, 1.0, and 1.5). A reduction in the elasticity modulus not only diminished the natural frequency of the harvester but also resulted in a slight rise in the output voltage. This can be assumed as a performance improvement criterion of such harvesters. The reduced elasticity modulus of the substrate layer at a ratio of 0.5 increased the maximum voltage to 10.609 V and reduced the natural frequency to 41.1 Hz.

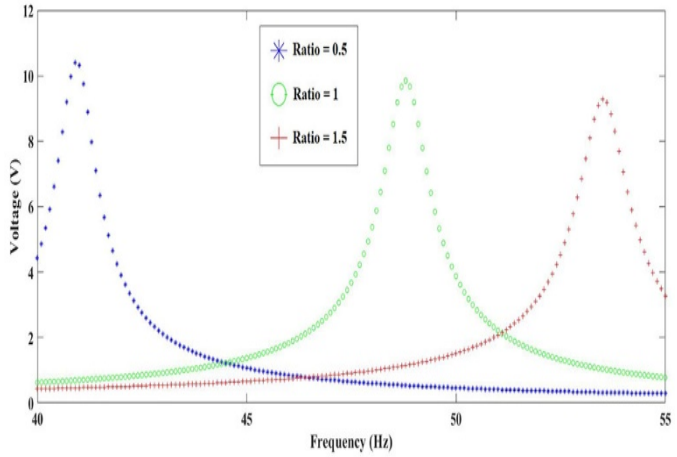

Figure 13. The voltage versus the frequency for variations in substrate Young's modulus through the analytical approach

Figure 14 shows the numerical results at 40-55 Hz in COMSOL. The numerical and analytical results show good agreement. Figure 15 plots the analytical voltage output at 37-60 Hz for piezoelectric layer elasticity moduli of 33, 66, and 99 GPa (ratios 0.5, 1.0, and 1.5). It was found that a reduction in the elasticity modulus of the piezoelectric layer reduced not only the maximum output voltage but also the natural frequency. This can be considered for reducing the natural frequency to the ambient excitation frequency range to improve harvester performance. A 50 % decrease in the elasticity modulus of the piezoelectric layer diminished the voltage to 9.2 V.

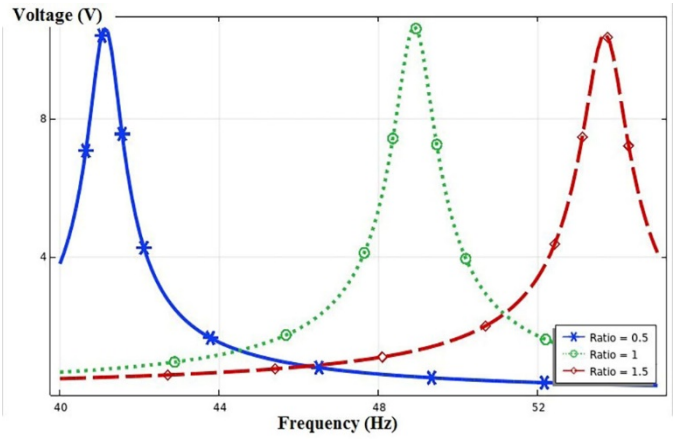

Figure 14. The voltage versus the frequency for variations in substrate Young's modulus from COMSOL Multiphysics

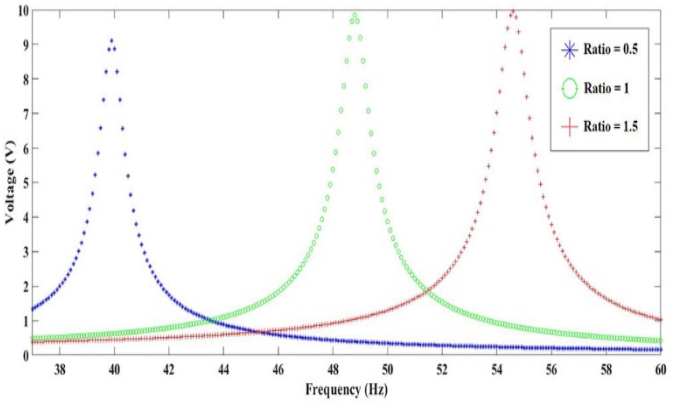

Figure 15. The voltage versus the frequency for variations in piezoelectric Young's modulus through the analytical approach

Figures 16 and 17 compare the analytical and numerical output voltages at 40-60 Hz for substrate layer densities of 3582.5, 7165, and 10747.5 kg/m^3 (ratios 0.5, 1.0, and 1.5). As can be seen, the analytical and numerical (COMSOL) results well agree. A rise in the substrate density was found to raise the output voltage and diminish the natural frequency. Thus, increased substrate density could be assumed as an effective measure to improve harvester performance. A 50 % rise in the substrate density increased the analytical output voltage to 12.4 V. Furthermore, factors of 0.5, 1.0, and 1.5 in the substrate density led to numerical output voltages of 7.928, 10.679, and 13.327 V and numerical natural frequencies of 57.1, 48.9, and 43.4 Hz, respectively.

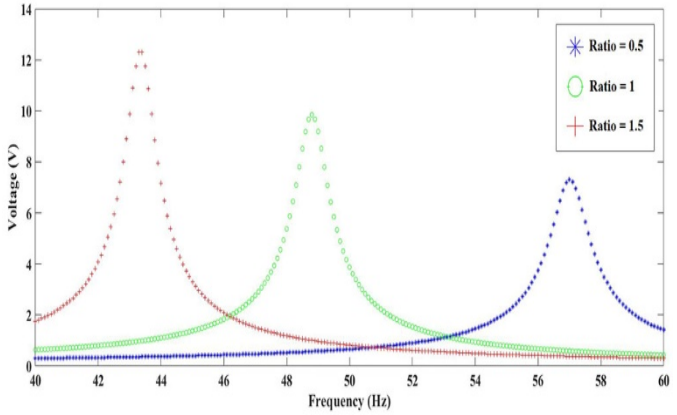

Figure 16. The voltage versus the frequency for variations in the density of the substrate layer through the analytical approach

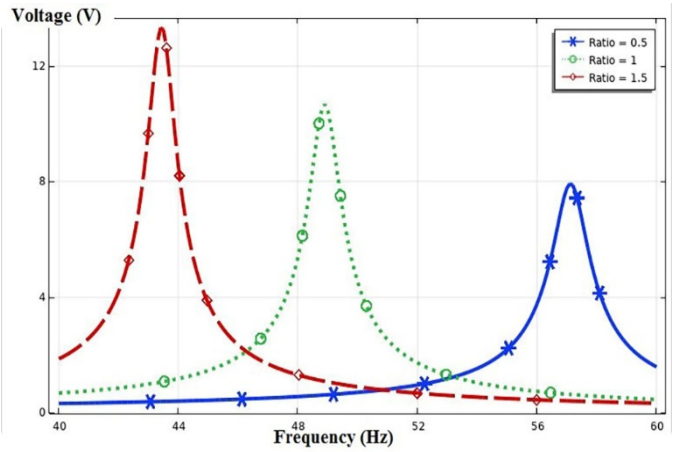

Figure 17. The voltage versus the frequency for variations in the density of the substrate layer from COMSOL Multiphysics

Figures 18 and 19 compare the analytical and numerical output voltages at 42-58 Hz for piezoelectric layer densities of 3900, 7800, and 11700 (ratios 0.5, 1.0, and 1.5). Likewise, an increase in the density of the piezoelectric layer not only increased the output voltage but also substantially reduced the natural frequency. Piezoelectric layer density ratios 0.5, 1.0, and 1.5 resulted in numerical output voltages of 8.283, 10.679, and 12.977 V and numerical natural frequencies of 55.8, 48.9, and 44.0, respectively. Table 3 shows variations in the output voltage and resonant frequency of the energy harvester for the two approaches of changing physical and geometric parameters.

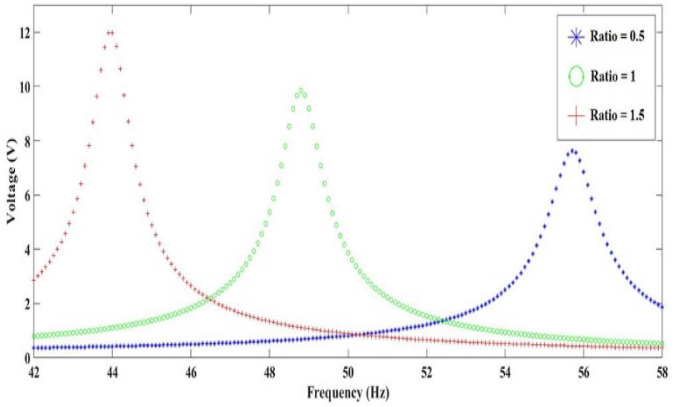

Figure 18. The voltage versus the frequency for variations in the density of the piezoelectric layer through the analytical approach

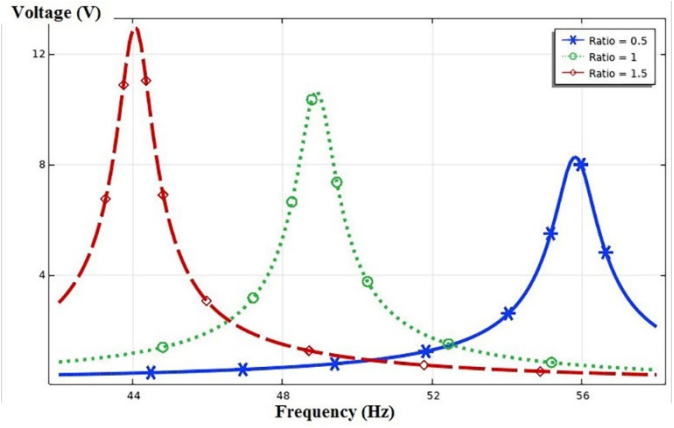

Figure 19. The voltage versus the frequency for variations in the density of the piezoelectric layer from COMSOL Multiphysics

Table 3. Percentage variations in the output voltage and resonant frequency of the cantilever energy scavenger due to changes in physical and geometric parameters

Parameter	Symbol/Unit	Quantity 1	Quantity 2	Quantity change (%)	Natural frequency change (%)	Output voltage change (%)
Length	l (mm)	50	100	+50	-152.57	+265.65
Piezoelectric thickness	h_p (mm)	0.2	0.4	+50	+25.71	+14.35
Substrate thickness	h_s (mm)	0.25	0.5	+50	+40.52	- 4.44
Piezoelectric density	ρ_p (kg/m^3)	3900	7800	+50	-12.37	+28.98
Substrate density	ρ_s (kg/m^3)	3582.5	7165	+50	-12.36	+34.68
Piezoelectric Young modulus	Y_p (Gpa)	33	66	+50	+22.29	+8.92
Substrate Young modulus	Y_s (Gpa)	50	100	+50	+18.98	+0.66

5. CONCLUSIONS

The performance of an energy scavenger was analyzed in this study by changing the geometrical and mechanical parameters of a unimorph cantilevered beam. The analysis of the energy harvester was done using COMSOL Multiphysics finite element software besides an analytical approach. According to the results, increasing the beam length led to a noticeable decrease in natural frequency, whereas the output voltage increased. Moreover, the output voltage decreased upon an increase in the thickness of the substrate layer. However, increasing the thickness of the piezoelectric layer increased the harvested energy. Furthermore, decreasing Young's modulus of the substrate layer or increasing Young's modulus of the piezoelectric layer increased the harvested energy. Finally, increasing the density of the piezoelectric layer or that of the substrate layer increased the output voltage and reduced the resonant frequency value. The results can be taken into account to design better energy harvesters and improve their performance.

6. ACKNOWLEDGEMENT

We thank our colleagues who provided insight and expertise that greatly assisted the research.

NOMENCLATURE

b	Beam width (m)
C	Damping
D_3	Electric displacement
d_{31}	Piezoelectric constant (pm/V)
E_3	Electric field
h	Beam thickness (m)
I	Moments of inertia
i	Electric current (A)
L	Beam length (m)
M	Internal bending moment
m	Mass per unit length of the beam
q	Electric charge
R_l	Load resistance (Ω)
S	Strain
T	Stress
v	Output voltage (V)
w	General motion of the beam
Y	Young's modulus (GPa)

Greek letters

$\emptyset_r$	Mass normalized eigenfunction
ϑ	Electromechanical coupling
ε_{33}^T	Permittivity (nF/m)
ρ	Density (kg/m^3)
λ	Dimensionless frequency number
η_r	Modal coordinate of the clamped-free beam

REFERENCES

1. Fakhzan, M.N. and Muthalif, A.G., "Harvesting vibration energy using piezoelectric material: Modeling, simulation and experimental verifications", ***Mechatronics***, Vol. 23, No. 1, (2013), 61-66. (https://doi.org/10.1016/J.MECHATRONICS.2012.10.009).
2. Yang, Z., Zhou, S., Zu, J. and Inman, D., "High-performance piezoelectric energy harvesters and their applications", ***Joule***, Vol. 2, No. 4, (2018), 642-697. (https://doi.org/10.1016/j.joule.2018.03.011).
3. Williams, C.B., Shearwood, C., Harradine, M.A., Mellor, P.H., Birch, T.S. and Yates, R.B., "Development of an electromagnetic micro-generator", ***Proceedings of IEEE-Circuits, Devices and Systems***, Vol. 148, No. 6, (2001), 337-342. (https://doi.org/10.1049/ip-cds:20010525).
4. Roundy, S., Wright, P.K. and Rabaey, J., "A study of low level vibrations as a power source for wireless sensor nodes", ***Computer Communications***, Vol. 26, No. 11, (2003), 1131-1144. (https://doi.org/10.1016/S0140-3664(02)00248-7).
5. Pradeesh, E.L. and Udhayakumar, S., "Effect of placement of piezoelectric material and proof mass on the performance of piezoelectric energy harvester", ***Mechanical Systems and Signal Processing***, Vol. 130, No. 1, (2019), 664-676. (https://doi.org/10.1016/j.ymssp.2019.05.044).
6. Eugeni, M., Elahi, H., Fune, F., Lampani, L., Mastroddi, F., Romano, G.P. and Gaudenzi, P., "Numerical and experimental investigation of piezoelectric energy harvester based on flag-flutter", ***Aerospace Science and Technology***, Vol. 11, No. 10, (2020), 933. (https://doi.org/10.3390/mi11100933).
7. Liu, Z., Cao, Y., Sha, A., Wang, H., Guo, L. and Hao, Y., "Energy harvesting array materials with thin piezoelectric plates for traffic data monitoring", ***Construction and Building Materials***, Vol. 302, No. 4, (2021), 124-147. (https://doi.org/10.1016/j.conbuildmat.2021.124147).
8. Zhao, Z., Dai, Y., Dou, S.X. and Liang, J., "Flexible nanogenerators for wearable electronic applications based on piezoelectric materials", ***Materials Today Energy***, Vol. 20, (2021), 100690. (https://doi.org/10.1016/j.mtener.2021.100690).
9. Su, H., Wang, X., Li, C., Wang, Z., Wu, Y., Zhang, J. and Zheng, H., "Enhanced energy harvesting ability of polydimethylsiloxane-$BaTiO_3$-based flexible piezoelectric nanogenerator for tactile imitation application", ***Nano Energy***, Vol. 83, (2021), 105809. (https://doi.org/10.1016/j.nanoen.2021.105809).
10. Nguyen, T.D., Deshmukh, N., Nagarah, J.M., Kramer, T., Purohit, P.K., Berry, M.J. and McAlpine, M.C., "Piezoelectric nanoribbons for monitoring cellular deformations", ***Nature Nanotechnology***, Vol. 10, No. 1038, (2012), 587-593. (https://doi.org/10.1038/nnano.2012.112).
11. Jamshidi, R. and Jafari, A.A., "Conical shell vibration control with distributed piezoelectric sensor and actuator layer", ***Composite Structures***, Vol. 117, No. 1016, (2021), 96-117. (https://doi.org/10.1016/j.isatra.2021.01.037).

12. Rui, X., Zeng, Z., Zhang, Y., Li, Y., Feng, H., Huang, X. and Sha, Z., "Design and experimental investigation of a self-tuning piezoelectric energy harvesting system for intelligent vehicle wheels", ***IEEE Transactions on Vehicular Technology***, Vol. 69, No. 2, (2020), 1440-1451 (https://doi.org/10.1109/TVT.2019.2959616).
13. Wang, K.F., Wang, B.L., Gao, Y. and Zhou, J.Y., "Nonlinear analysis of piezoelectric wind energy harvesters with different geometrical shapes", ***Archive of Applied Mechanics***, Vol. 90, No. 2, (2020), 721-736. (https://doi.org/10.1007/s00419-019-01636-8).
14. Pradeesh, E.L., Udhayakumar, S. and Sathishkumar, C., "Investigation on various beam geometries for piezoelectric energy harvester with two serially mounted piezoelectric materials", ***SN Applied Sciences***, Vol. 1, No.1648, (2019), 1-11. (https://doi.org/10.1007/s42452-019-1709-4).
15. Zhang, S., Liu, Y., Deng, J., Tian, X. and Gao, X., "Development of a two-DOF inertial rotary motor using a piezoelectric actuator constructed on four bimorphs", ***Mechanical Systems and Signal Processing***, Vol. 149, (2021). (https://doi.org/10.1016/j.ymssp.2020.107213).
16. Moon, K., Choe, J., Kim, H., Ahn, D. and Jeong, J., "A method of broadening the bandwidth by tuning the proof mass in a piezoelectric energy harvesting cantilever", ***Sensors and Actuators, A: Physical***, Vol. 276, No. 1648, (2018), 17-25. (https://doi.org/10.1016/j.sna.2018.04.004).
17. Zhang, G., Gao, S., Liu, H. and Niu, S., "A low frequency piezoelectric energy harvester with trapezoidal cantilever beam: theory and experiment", ***Microsystem Technologies***, Vol. 23, (2017), 3457-3466. (https://doi.org/10.1007/s00542-016-3224-5).
18. Karadag, C.V., Ertarla, S., Topaloglu, N. and Okyar, A.F., "Optimization of beam profiles for improved piezoelectric energy harvesting efficiency", ***Structural and Multidisciplinary Optimization***, Vol. 63, (2021), 631-643. (https://doi.org/10.1007/s00158-020-02714-0).
19. Lee, M.S., Kim, C.I., Park, W.I., Cho, J.H., Paik, J.H. and Jeong, Y.H., "Energy harvesting performance of unimorph piezoelectric cantilever generator using interdigitated electrode lead zirconate titanate laminate", ***Energy***, Vol. 179, (2019), 373-382. (https://doi.org/10.1016/j.energy.2019.04.215).
20. Alameh, A.H., Gratuze, M. and Nabki, F., "Impact of geometry on the performance of cantilever-based piezoelectric vibration energy harvesters", ***IEEE Sensors Journal***, Vol. 19, No. 22, (2019), 10316-10326. (https://doi.org/10.1109/JSEN.2019.2932341).
21. Rua Taborda, M.I., Elissalde, C., Chung, U.C., Maglione, M., Fernandes, E., Salehian, A. and Debéda, H., "Key features in the development of unimorph stainless steel cantilever with screen-printed PZT dedicated to energy harvesting applications", ***International Journal of Applied Ceramic Technology***, Vol. 17, No. 6, (2020), 2533-2544. (https://doi.org/10.1111/ijac.13588).
22. Ahoor, Z.H., Ghafarirad, H. and Zareinejad, M., "Nonlinear dynamic modeling of bimorph piezoelectric actuators using modified constitutive equations caused by material nonlinearity", ***Mechanics of Advanced Materials and Structures***, Vol. 28, No. 8, (2021), 763-773. (https://doi.org/10.1080/15376494.2019.1590885).
23. Erturk, A. and Inman, D.J., "A distributed parameter electromechanical model for cantilevered piezoelectric energy harvesters", ***Journal of Vibration and Acoustics***, Vol. 130, No. 4, (2008), 1-15. (https://doi.org/10.1115/1.2890402).
24. Rahimzadeh, M., Samadi, H. and Mohammadi, N.S., "Analysis of energy harvesting enhancement in piezoelectric unimorph cantilevers", ***Sensors***, Vol. 21, No. 24, (2021), 1-16. (https://doi.org/10.3390/s21248463).